Heterogeneous Influence of Glacier Morphology on the Mass Balance Variability in High Mountain Asia

F. Brun, P. Wagnon, Etienne Berthier, V. Jomelli, S. Maharjan, F. Shrestha, P. Kraaijenbrink

▶ **To cite this version:**

F. Brun, P. Wagnon, Etienne Berthier, V. Jomelli, S. Maharjan, et al.. Heterogeneous Influence of Glacier Morphology on the Mass Balance Variability in High Mountain Asia. Journal of Geophysical Research: Earth Surface, 2019, 124 (6), pp.1331-1345. 10.1029/2018JF004838 . hal-02989853v2

HAL Id: hal-02989853
https://hal.science/hal-02989853v2

Submitted on 8 Apr 2021

HAL is a multi-disciplinary open access archive for the deposit and dissemination of scientific research documents, whether they are published or not. The documents may come from teaching and research institutions in France or abroad, or from public or private research centers.

L'archive ouverte pluridisciplinaire **HAL**, est destinée au dépôt et à la diffusion de documents scientifiques de niveau recherche, publiés ou non, émanant des établissements d'enseignement et de recherche français ou étrangers, des laboratoires publics ou privés.

Check for updates

JGR Earth Surface

RESEARCH ARTICLE
10.1029/2018JF004838

Heterogeneous Influence of Glacier Morphology on the Mass Balance Variability in High Mountain Asia

F. Brun[1,2], P. Wagnon[1], E. Berthier[2], V. Jomelli[3], S. B. Maharjan[4], F. Shrestha[4], and P. D. A. Kraaijenbrink[5]

[1]Univ. Grenoble Alpes, CNRS, IRD, Grenoble INP, IGE, Grenoble, France, [2]LEGOS, Université de Toulouse, CNES, CNRS, IRD, UPS, Toulouse, France, [3]Université Paris 1 Panthéon-Sorbonne, CNRS Laboratoire de Géographie Physique, Meudon, France, [4]International Centre for Integrated Mountain Development (ICIMOD), Kathmandu, Nepal, [5]Department of Physical Geography, Faculty of Geosciences, Utrecht University, Utrecht, The Netherlands

Abstract We investigate the control of the morphological variables on the 2000–2016 glacier-wide mass balances of 6,470 individual glaciers of High Mountain Asia. We separate the data set into 12 regions assumed to be climatically homogeneous. We find that the slope of the glacier tongue, mean glacier elevation, percentage of supraglacial debris cover, and avalanche contributing area all together explain a maximum of 48% and a minimum of 8% of the glacier-wide mass balance variability, within a given region. The best predictors of the glacier-wide mass balance are the slope of the glacier tongue and the mean glacier elevation for most regions, with the notable exception of the inner Tibetan Plateau. Glacier-wide mass balances do not differ significantly between debris-free and debris-covered glaciers in 7 of the 12 regions analyzed. Lake-terminating glaciers have more negative mass balances than the regional averages, the influence of lakes being stronger on small glaciers than on large glaciers.

Key Points:
- Debris-free and debris-covered glaciers have statistically indistinguishable glacier-wide mass balances over 2000–2016
- Lake-terminating glaciers on average have more negative mass balances than land-terminating glaciers
- Morphological variables explain 8% to 48% of the variance of High Mountain Asia glacier mass balances for the period 2000–2016

Supporting Information:
- Supporting Information S1

Correspondence to:
F. Brun,
f.brun-barriere@uu.nl

Citation:
Brun, F., Wagnon, P., Berthier, E., Jomelli, V., Maharjan, S. B., Shrestha, F., & Kraaijenbrink, P. D. A. (2019). Heterogeneous influence of glacier morphology on the mass balance variability in High Mountain Asia. *Journal of Geophysical Research: Earth Surface*, *124*, 1331–1345. https://doi.org/10.1029/2018JF004838

Received 6 AUG 2018
Accepted 2 APR 2019
Accepted article online 8 APR 2019
Published online 3 JUN 2019

©2019. American Geophysical Union. All Rights Reserved.

1. Introduction

Glacier mass balance is widely recognized as a sensitive indicator of climate change (e.g., Bojinski et al., 2014). Recent studies showed the contrasted glacier mass changes at the scale of the Pamir-Karakoram-Himalaya and even at the scale of the entire High Mountain Asia (HMA) for the beginning of the 21st century (e.g., Brun et al., 2017; Gardelle et al., 2013; Gardner et al., 2013; Kääb et al., 2015). Causes of these spatiotemporal changes are still not fully understood, because the climate variability is not well constrained and because the response of each individual glacier to climate variability is modulated by its morphology, further complicating the interpretation of glacier mass changes. Heterogeneous climatology (Maussion et al., 2014) could be responsible for various glacier mass balance sensitivities to temperature, explaining partly the regional pattern of recent glacier mass changes (Sakai & Fujita, 2017). Other studies highlighted the role of heterogeneity of climate change itself, in explaining the regional pattern of glacier mass balance (e.g., Forsythe et al., 2017; Kapnick et al., 2014). The morphology of the glaciers and their catchments and the abundance of supraglacial debris show large variations in HMA and may also explain part of the variability of glacier mass balance.

Previous studies showed that, in the European Alps, annual fluctuations of glacier-wide mass balance are strongly correlated in a given region (e.g., Vincent et al., 2017) and are related to meteorological annual fluctuations (e.g., Rabatel et al., 2013). Nevertheless, multidecadal averages of individual glacier mass balances are linked to glacier morphology (e.g., Fischer et al., 2015; Huss, 2012; Huss et al., 2012; Paul & Haeberli, 2008; Rabatel et al., 2013, 2016). For instance, Huss (2012) found that a combination of six morphological variables explained 51% of the glacier mass balance variance. For HMA, Salerno et al. (2017) conducted a statistical analysis of the thinning rates of glaciers in the Everest region, in relationship with morphological variables. They found that the slope of the glacier tongue was the main morphological variable controlling the glacier thickness changes, and they suggested that this was partially explained by preferential development of glacial ponds on shallow slopes (e.g., Quincey et al., 2007). To our knowledge, this is the only study investigating the link between glacier thickness changes and morphological variables in HMA, and it is limited to a small region (360 km^2 of glacierized area).

The influence of debris at the surface of many HMA glaciers is the subject of an ongoing debate and requires more investigation at large spatial scale. Geodetic studies suggested similar thinning rates over debris-free

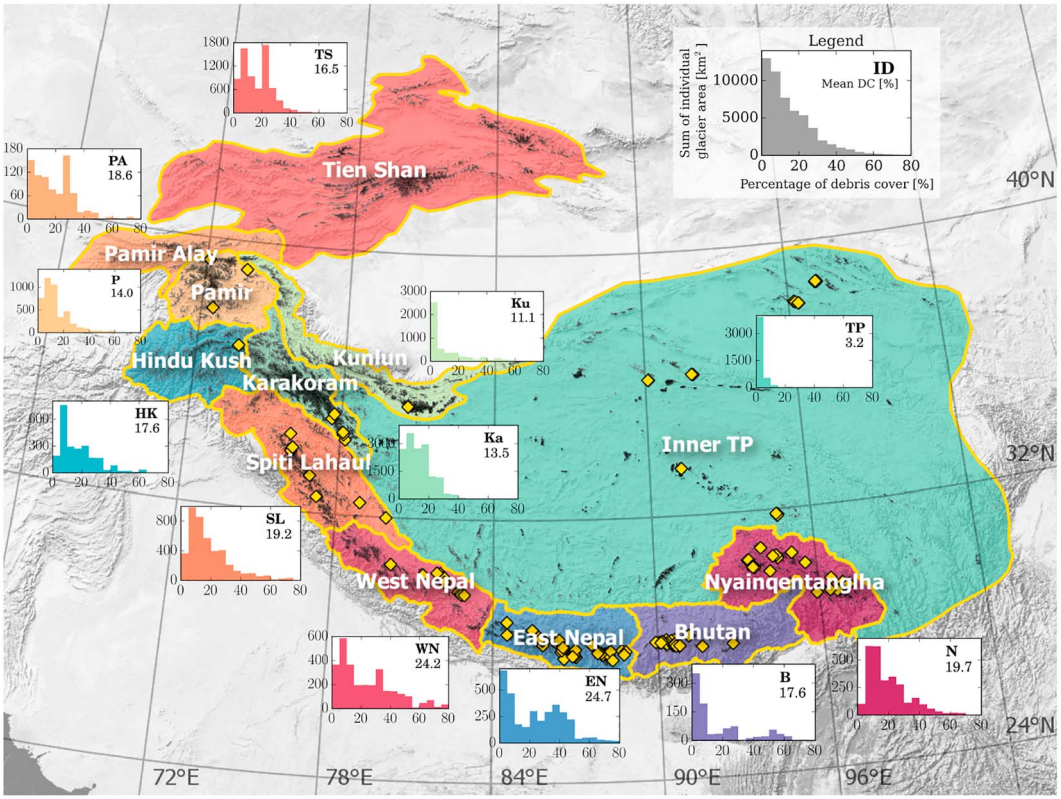

Figure 1. Distribution of the debris-covered and lake-terminating glaciers in High Mountain Asia. The histograms represent the distributions of the supraglacial debris cover percentage. The number is the percentage of the total glacierized area which is debris covered. The yellow diamonds represent the locations of the lake-terminating glaciers studied here.

and debris-covered ice for ablation tongues in the same elevation range (Gardelle et al., 2012, 2013; Kääb et al., 2012, Nuimura et al., 2012). This finding is in apparent contradiction with the reduced ablation expected for ice beneath a thick debris layer (e.g., Nicholson & Benn, 2006). Salerno et al. (2017) also investigated this question and found that the presence of supraglacial debris cover was not a significant contributor to differences in thinning rates among the studied glaciers. However, they examined a restricted sample of glaciers ($n = 28$) and analyzed only tongue-averaged thinning rates, which are less straightforward to interpret than glacier-wide mass balances as they result from the sum of surface mass balance and emergence velocity (e.g., Cuffey & Paterson, 2010). Consequently, there is a need to test this hypothesis over the glacier-wide mass balances of a larger number of glaciers and in different climate contexts.

Furthermore, the development of proglacial lakes at glacier termini is a topic of interest in HMA, as they are associated with enhanced glacier mass loss through subaqueous melting (e.g., Röhl, 2006), accelerated ice flows (e.g., King et al., 2018), and with potential hazardous glacier lake outburst floods (GLOFs; e.g., Haritashya et al., 2018). Compared with land-terminating glaciers, lake-terminating glaciers shrink faster in Sikkim (Basnett et al., 2013), have more negative rates of elevation changes in Bhutan, Everest region, and West Nepal (Gardelle et al., 2013), and have more negative mass balances in the Everest region (King et al., 2017). Terminal lakes develop when supraglacial ponds coalesce into a single lake dammed by a terminal moraine (e.g., Benn et al., 2012; Thompson et al., 2012). Eventually, the terminal lake enhances the frontal ablation by dynamic thinning, calving, and thermo-erosion (e.g., Benn et al., 2012). To our knowledge, the only study quantifying the influence of terminal lake on glacier-wide mass balance was conducted on 32 glaciers (nine of them being lake-terminating glaciers) and restricted to the Everest region (King et al., 2017).

In this study, we build upon the work of Salerno et al. (2017) and King et al. (2017). We extend them by adding additional variables, such as the avalanche contributing area, and we extend the analysis to the entire HMA, by analyzing 6,470 individual glacier (>2 km^2) mass changes in relationship with morphological variables. For each of the 12 regions defined in Brun et al. (2017) and shown in Figure 1, that is, Bhutan (B), East

Nepal (EN), Hindu Kush (HK), Inner Tibetan Plateau (TP), Karakoram (Ka), Kunlun (Ku), Nyainqentanglha (N), Pamir (P), Pamir Alay (PA), Spiti Lahaul (SL), Tien Shan (TS), and West Nepal (WN), we test whether supraglacial debris cover reduces mass loss, whether lake-terminating glaciers have more negative mass balance, and we assess the part of the variance of glacier mass balance explained by the morphological variables. As we focus on debris-covered glaciers, we also extend the work of Scherler et al. (2011a), to assess the morphological specificities of debris-covered glaciers.

2. Data and Methods

2.1. Glacier-Wide Mass Balance and Morphological Data

The glacier-wide geodetic mass balance, $\dot{M}$ (named glacier mass balance for simplicity hereafter), data are calculated from the rate of elevation change, extracted from a linear fit of multitemporal digital elevation models (DEMs) obtained from the Advanced Spaceborne Thermal Emission and Reflection Radiometer (ASTER), as described in Brun et al. (2017). Only glaciers larger than 2 km^2 are included to limit the error on the glacier mass balance, which decreases with increasing glacier area (Rolstad et al., 2009). Glaciers with less than 70% of reliable elevation change rates are excluded from the analysis, leading to a total number of 6,480 glaciers. Even though the majority of the ~95,000 glaciers of HMA are excluded from this analysis due to their small size, our sample still represents 54% of the total glacierized area of the HMA (Pfeffer et al., 2014). The glacier mass balances are calculated using the RGI 5.0 glacier mask (Pfeffer et al., 2014), which is based mostly on satellite images acquired in the early 2000s. For a discussion about the influence of the uncertainties of the glacier inventory on the geodetic mass balance, the reader is referred to the supplementary of Brun et al. (2017). The individual glacier mass balances have a median uncertainty of ±0.22 m water equivalent (w.e.)/a, ranging from a minimum of ±0.14 to a maximum of ±0.89 m w.e./a (Brun et al., 2017).

In this study we explore glacier morphological variables (area, aspect, mean slope, slope of the lowest 20 % [tongue slope], mean elevation [mean elev.], median elevation, minimum elevation, maximum elevation, area percentage of supraglacial debris cover [DC], and avalanche contributing area [contrib. area]) found to have an influence on mass balance in previous studies (e.g., Fischer et al., 2015; Huss, 2012; Salerno et al., 2017). The glacier morphological variables are calculated from the gridded debris cover classification and elevation raster by Kraaijenbrink et al. (2017), which are clipped to the RGI 5.0 glacier extents and have a resolution of 30 m. All the areas are calculated as planar areas (Cogley et al., 2011). The glacier mean aspect (in degree) is calculated as the vector average of the aspect of individual pixels in order to avoid the typical problems due to direct averaging of discontinuous aspect values. The mean slope (in degree) is calculated as direct average of the slope of individual pixels and the tongue slope as the average of the slope of the pixels with an elevation below the twentieth percentile of the elevation for this glacier. The area percentage of supraglacial debris cover is calculated as the ratio of the glacier area classified as debris or as supraglacial ponds divided by the total glacier area. The avalanche contributing area (in square kilometers) is defined as the nonglacierized area in the catchment upstream of the glacier median elevation with a slope steeper than 30° (Figure 2). The catchment upstream of the median glacier elevation is calculated based on the Shuttle Radar Topographic Mission (SRTM) 30-m void-filled DEM (Farr et al., 2007) and the upslope area module (Freeman, 1991) implemented in the SAGA software (Conrad et al., 2015). More sophisticated approaches exist in the literature (e.g., Bernhardt & Schulz, 2010), but, even though the avalanche contributing area significantly depends on the slope threshold, the correlation between this area and the percentage of debris cover showed a very weak sensitivity to the slope threshold. Consequently, we used a 30° threshold. Figure 2 illustrates these different areas for the example of Khumbu Glacier (RGI Id 5.0-15.03733). Through the data analysis, we detected some obvious outliers (10 glaciers), like, for example, glaciers with unrealistic low minimum elevation. These errors come from artifacts in the SRTM DEM, and we exclude these glaciers from the analysis, leading to a final number of 6,470 glaciers.

2.2. Classification of Debris-Covered and Debris-Free Glaciers

We propose to classify glaciers into two separate categories (debris-covered glaciers and debris-free glaciers), based on the area percentage of supraglacial debris cover. To our knowledge, there is no standard widely accepted definition of what is a debris-covered glacier. For instance, Xiang et al. (2018) use a 5% threshold for the debris cover area fraction, whereas Janke et al. (2015) use a 25% threshold to define the debris-covered glaciers. We determine an optimal threshold of 19% of debris cover, based on 100 randomly selected glaciers classified by five operators, as described in supporting information Text S1 (Herreid & Pellicciotti, 2018)

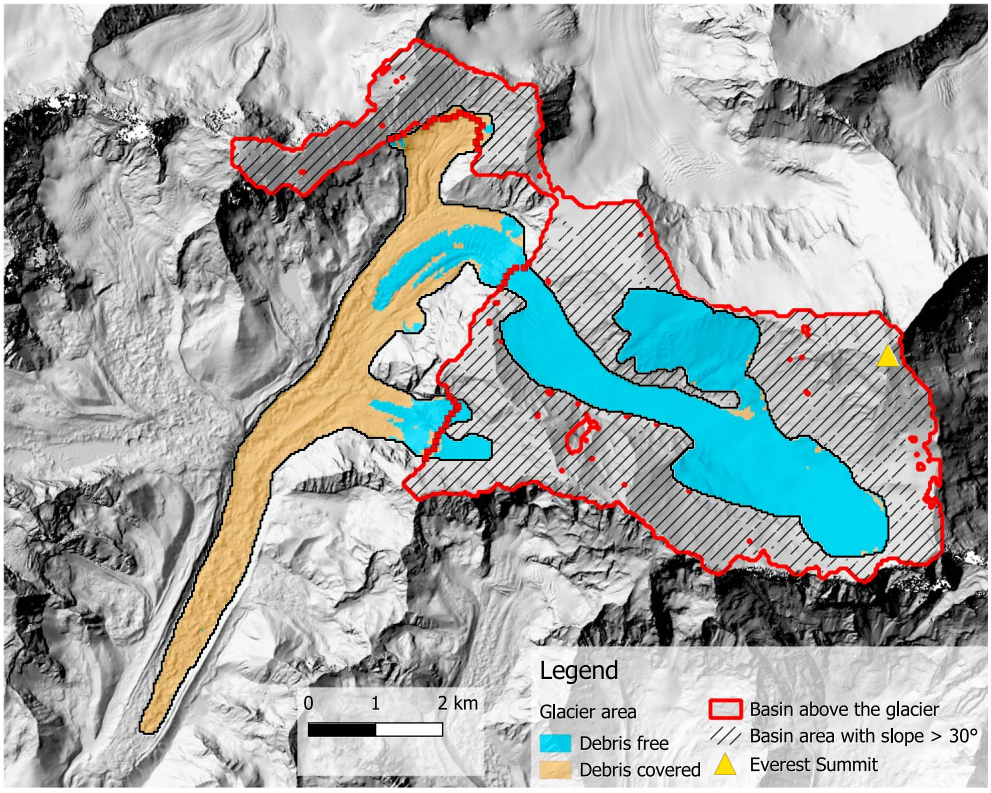

Figure 2. Example of the calculation of the avalanche contributing area for Khumbu Glacier (RGI ID 15.03733). The glacier area is classified either as debris-covered or debris-free following Kraaijenbrink et al. (2017), the basin above the glacier is the area (in gray) upstream of the glacier area above the glacier median elevation (red dashed line), and the avalanche accumulating area is the parts of this basin where the slopes are steeper than 30 (hatched area). The background is a hillshade derived from the High Mountain Asia digital elevation model (Shean, 2017).

and Figures S1 and S2. It is noteworthy that this distinction is arbitrary, as there is a continuum between debris-covered and debris-free glaciers. However, we find useful to make this categorization, as it simplifies the analysis. In our comparison between debris-covered and debris-free glaciers, we assess the sensitivity of the glacier-wide mass balances aggregated by glacier type to this threshold by testing 14% and 24% thresholds.

2.3. Classification of Lake-Terminating and Land-Terminating Glaciers

We automatically select the glaciers in contact with lakes (within a 50-m buffer) from a lake inventory produced by the International Centre for Integrated Mountain Development (Maharjan et al., 2018) and the glacial lake inventory produced by Zhang et al. (2017). Both inventories are based on Landsat images collected in the early 2000s, with a focus on the 2004–2007 period for the ICIMOD inventory. Then from visual inspection of satellite images accessed through Google Earth, we retain 131 glaciers, which are actually lake-terminating glaciers. The lake inventory does not cover the Tien Shan and Pamir Alay regions, and our samples include only 1, 1, 3, and 5 lake-terminating glaciers in Kunlun, Hindu Kush, Pamir, and Karakoram, respectively. Consequently, we focus the analysis on the six remaining regions: Bhutan (21 lakes), East Nepal (47 lakes), inner Tibetan Plateau (16 lakes), Spiti Lahaul (7 lakes), West Nepal (11 lakes), and Nyainqentanglha (19 lakes). Eight of these glaciers are excluded from the analysis because we could not calculate their mass balance from ASTER DEMs (because they have less than 70 % of reliable rate of elevation change coverage).

2.4. Linear Analysis and Multivariate Linear Model

We perform univariate linear analysis, by calculating the Pearson's correlation coefficients and associated p values for all the 2-by-2 combinations of available variables as well as, for some of them, their exponential and logarithmic values (Tables S1–S12). We also implemented a simple multivariate linear model to deter-

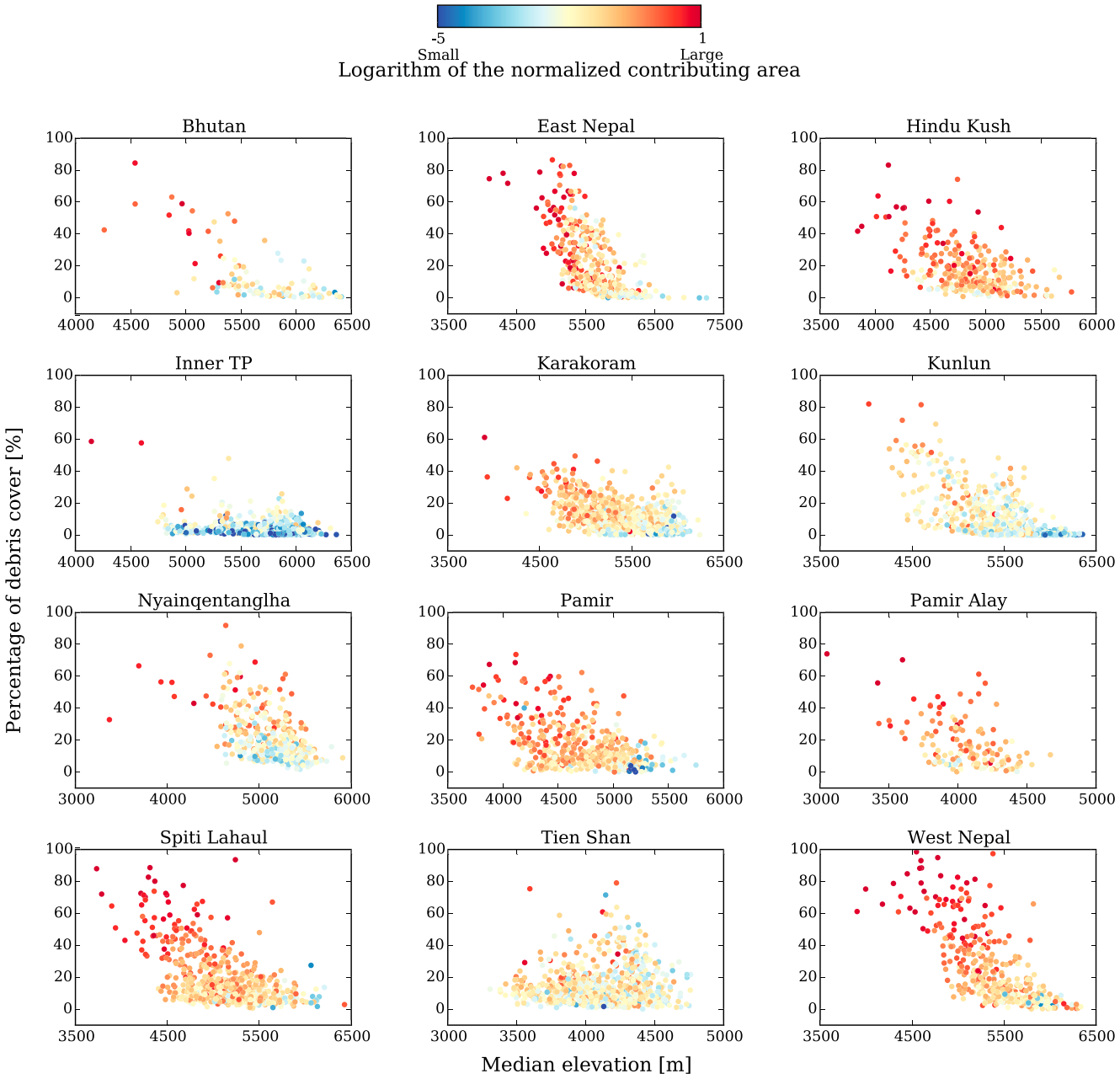

Figure 3. Percentage of the glacier supraglacial debris cover as a function of the glacier median elevation. The dots represent individual glaciers and are colorized accordingly to the logarithm of their normalized avalanche contributing area, defined as the ratio of the avalanche contributing area divided by the glacier area.

mine the best predictors (and combination of predictors) of the glacier mass balance ($\dot{M}$) variability. This model aims at finding the set of coefficients ($\alpha_1, \alpha_2, \ldots \alpha_n$), which explains a maximum of the mass balance variance, when multiplying the predictors ($x_1, x_2, \ldots x_n$), such as

$$\dot{M} = \alpha_1 x_1 + \alpha_2 x_2 + \ldots + \alpha_n x_n. \quad (1)$$

We worked with standardized predictors and standardized $\dot{M}$ to allow for a direct comparison between the coefficients α_i. The standardized predictor $x_{i,s}$, derived from the variable x_i, is defined as

$$x_{i,s} = \frac{x_i - \overline{x_i}}{\sqrt{\mathrm{V}(x_i)}}, \quad (2)$$

where $\overline{x_i}$ is the variable regional average and $\mathrm{V}(x_i)$ is its regional variance.

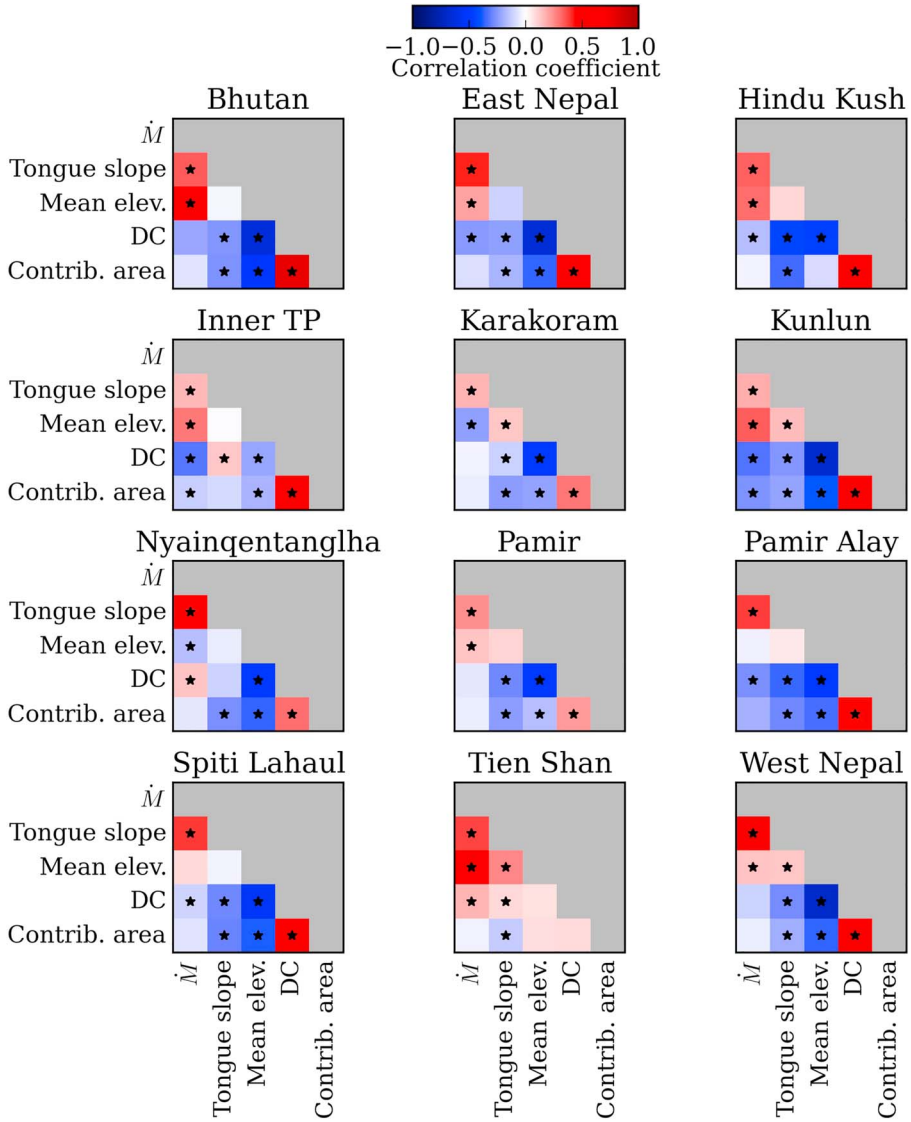

Figure 4. Pearson correlation coefficients between selected variables. The ⋆ denotes correlation significant at $p < 0.01$. DC = debris cover; TP = Inner Tibetan Plateau.

We explore the morphological variables that explain the maximum of the variance, but the selection of the different variables to include in the multivariate linear model is subjective, and we could not find an optimal combination of variables which minimized the Akaike (1974) Information Criterion (the Akaike Information Criterion is a metric that penalizes models with a large number of parameters) while maximizing the explained variance (R^2) of $\dot{M}$ for all the regions simultaneously. Similarly, standard approaches such as the forward selection and backward elimination, which consist in an evaluation of the model after adding or removing variables until an optimal combination is reached (e.g., Hocking, 1976), give different results for different regions, mainly because some variables were very redundant (e.g., the mean and the median elevation). These attempts to select the best performing model in an objective way were not successful. Instead, we favor variables that are often selected in the literature, such as the supraglacial debris cover or the avalanche contributing area (Huss et al., 2012; Salerno et al., 2017). We subjectively choose the final variables analyzed hereafter and retain the tongue slope, the mean elevation, the area percentage of supraglacial debris cover, and the avalanche contributing area.

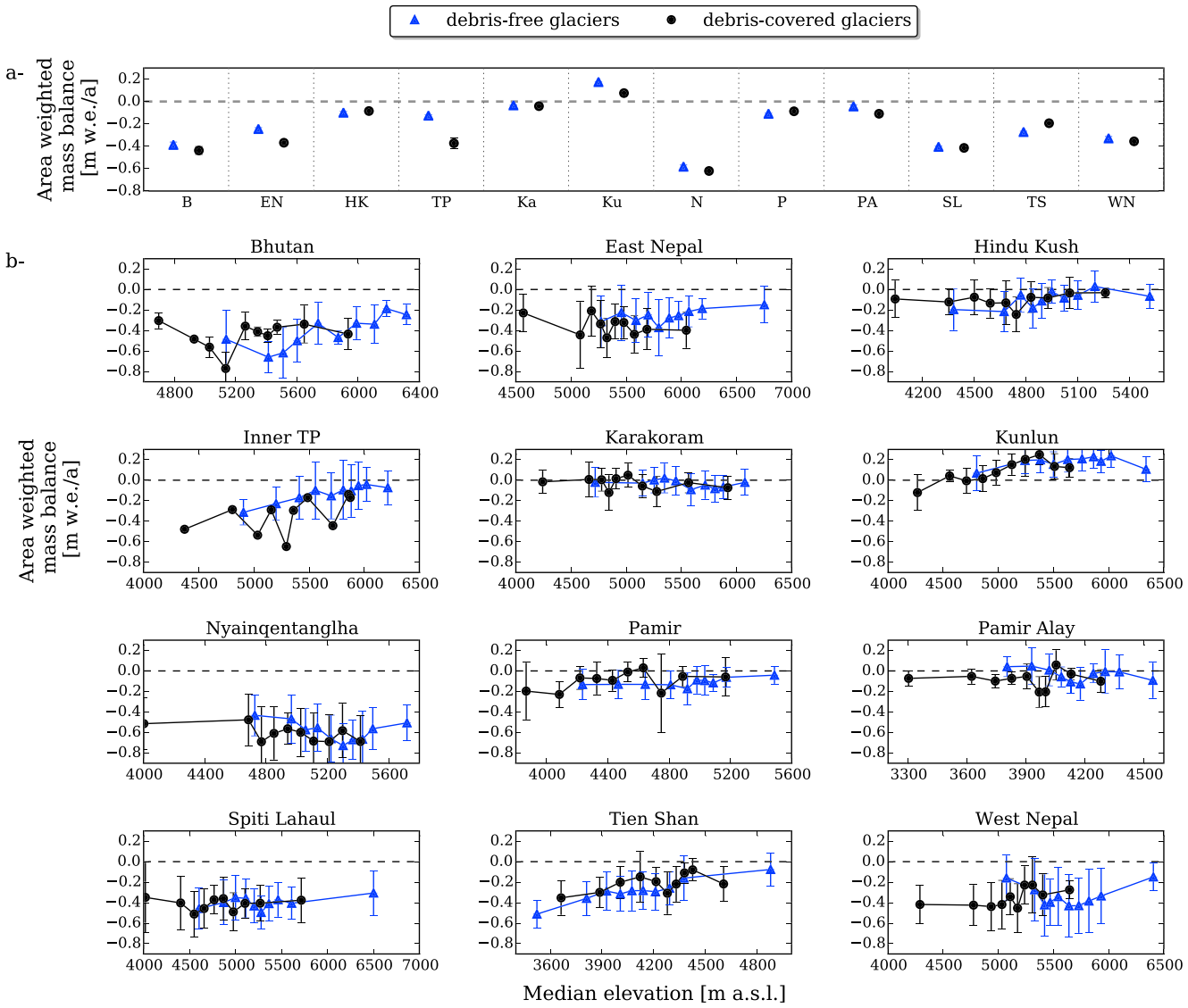

Figure 5. Glacier mass balances for debris-covered and debris-free glaciers; (a) regional averages and (b) glaciers grouped by 10 percentiles of glacier mean elevation. The error bars represent the standard error on the mean, note that for the regional averages, the dot size is most of the time larger than the error bars. The standard errors are smaller than the regional uncertainties of the glacier mass balance from Brun et al. (2017), because the latter takes into account the spatial correlation, whereas the standard error is used here to quantify the dispersion of the glacier population. TP = Inner Tibetan Plateau.

3. Results

3.1. Contrasted Glacier Morphologies in the Different Regions

Our analysis shows that the different regions have varying supraglacial debris cover, with mean percentage of supraglacial debris cover ranging from 3.2% in the inner TP to 24.7% in the East Nepal (Figure 1). With a threshold of 19% to distinguish between debris-free and debris-covered glaciers, we find that debris-covered glaciers occupy between 1.5% of the total glacierized area in the inner TP and 56.7% in the East Nepal (Figure 1). The extent of supraglacial debris cover is controlled by the local relief, and in particular the area occupied by ice-free terrain above the glacier, which contributes to the debris supply (Scherler et al., 2011a). We extend the analysis of Scherler et al. (2011a), which cover only a limited number of glaciers (287) over selected regions (Hindu Kush, Karakoram, Kunlun, Spiti Lahaul, West Nepal, East Nepal, and Bhutan), to our sample of 6,470 glaciers, and we search for the morphological variables that could explain part of the variability of the supraglacial debris cover. In all regions except Tien Shan, the percentage of supraglacial debris cover increases with the avalanche contributing area, with a positive correlation with R ranging from 0.23 to 0.77 and $p < 0.001$ (Figure 4 and Tables S1–S12). It decreases with increasing median elevation,

Table 1
Mean of the Regional Mass Balance for Debris-Free ($\dot{M}_{DF}$) and Debris-Covered ($\dot{M}_{DC}$) Glaciers for Each Region in Meter Water Equivalent Per Annum

Region	B	EN	HK	TP	Ka	Ku	N	P	PA	SL	TS	WN
$\dot{M}_{DF}$	−0.39	−0.25	−0.10	−0.13	−0.04	0.17	−0.58	−0.11	−0.04	−0.41	−0.27	−0.33
Err. std. $\dot{M}_{DF}$	0.03	0.01	0.01	0.01	0.00	0.01	0.02	0.01	0.02	0.01	0.01	0.02
$\dot{M}_{DC}$	−0.44	−0.37	−0.08	−0.37	−0.04	0.08	−0.62	−0.09	−0.11	−0.41	−0.19	−0.36
Err. std. $\dot{M}_{DC}$	0.04	0.02	0.02	0.05	0.01	0.01	0.02	0.02	0.02	0.02	0.02	0.02
N_{DF}	80	271	196	719	1,039	565	230	419	94	501	701	243
N_{DC}	24	161	100	11	138	120	161	132	47	179	175	173

Note. The standard error is calculated as the standard deviation of $\dot{M}$ in meter water equivalent per annum divided by the square root of the number of glaciers in each subgroup (N_{DF} and N_{DC}). Note that the standard errors are smaller than the regional uncertainties of the glacier mass balance from Brun et al. (2017), because the latter takes into account the spatial correlation, whereas the standard error is used here to quantify the dispersion of the glacier population.

with a negative correlation with R ranging from −0.69 to −0.22 and $p < 0.001$ (Figure 4 and Tables S1–S12). Indeed, the insulating effect of debris allows for the existence of debris-covered tongues at low elevation (Figure 3). Very few glaciers are debris covered in the inner TP, where glaciers are often surrounded by gentler slopes than the glaciers in other regions of HMA. Glaciers located in Tien Shan do not follow the same distribution as in the other regions, as the supraglacial debris cover is neither related with the median elevation nor with the avalanche contributing area (Figure 3). With the exception of Inner TP and Tien Shan, we also found a significant negative correlation between the percentage of supraglacial debris cover and the tongue slope, with R reaching a minimum of −0.44 and various levels of significance (Figure 4 and Tables S1–S12). Other variables, such as glacier area or mean aspect, do not show systematic correlations with the percentage of supraglacial debris cover and exhibit large region to region differences (Tables S1–S12).

The lake-terminating glaciers are mostly located in the southeastern margin of the HMA (Figure 1). The sample size is not large enough to perform a robust statistical analysis.

3.2. Influence of the Supraglacial Debris Cover on the Mass Balance Variability

In this section, we test the influence of the percentage of supraglacial debris cover on the mass balance variability in two ways: First, we test the correlation between the percentage of supraglacial debris cover and the mass balance, and second, we test the difference between two populations of glaciers (debris-free vs. debris-covered) in terms of region-wide mass balances.

First, we tested whether the supraglacial debris cover reduces the glacier mass losses. This hypothesis is rejected as a positive and significant correlation between $\dot{M}$ and DC is found only for Tien Shan and Nyainqentanglha (Figure 4 and Tables S1–S12). For all the other regions, the correlation was either negative or not significant.

Second, in terms of regional area weighted averages, debris-covered glaciers have a $\dot{M}$ significantly (i.e., with a 95% confidence t test) more negative than debris-free glaciers in East Nepal, inner TP, Kunlun, and Pamir Alay, with an absolute value of the difference ranging from 0.06 to 0.24 m w.e./a (Figure 5a and Table 1). The later value corresponds to the inner TP, where we find only 11 debris-covered glaciers and consequently should be interpreted with caution. In Tien Shan, it is the opposite (with the absolute value of the difference being 0.08 m w.e./a), and for the remaining regions (seven in total), the differences are not significant.

When we group glaciers by mean elevations to calculate an averaged $\dot{M}$ for each 10 percentile of mean elevation (Figure 5b), slight statistically nonsignificant differences are apparent between regions. For instance, in East Nepal, Nyainqentanglha, Pamir Alay, and in inner TP, the debris-covered glaciers have more negative $\dot{M}$ at the same elevation, whereas it is the opposite for Bhutan, Pamir, and Tien Shan.

These results are not very sensitive to the threshold used to discriminate between debris-free and debris-covered glaciers. Although the altitudinal distribution of debris-covered and debris-free glaciers is strongly modified if we use a threshold of 14% or 24% to discriminate debris-covered and debris-free glaciers (Figures S3 and S4), the differences of $\dot{M}$ between debris-free and debris-covered glaciers are close to the 19% threshold differences (less than ±0.05 m w.e./a).

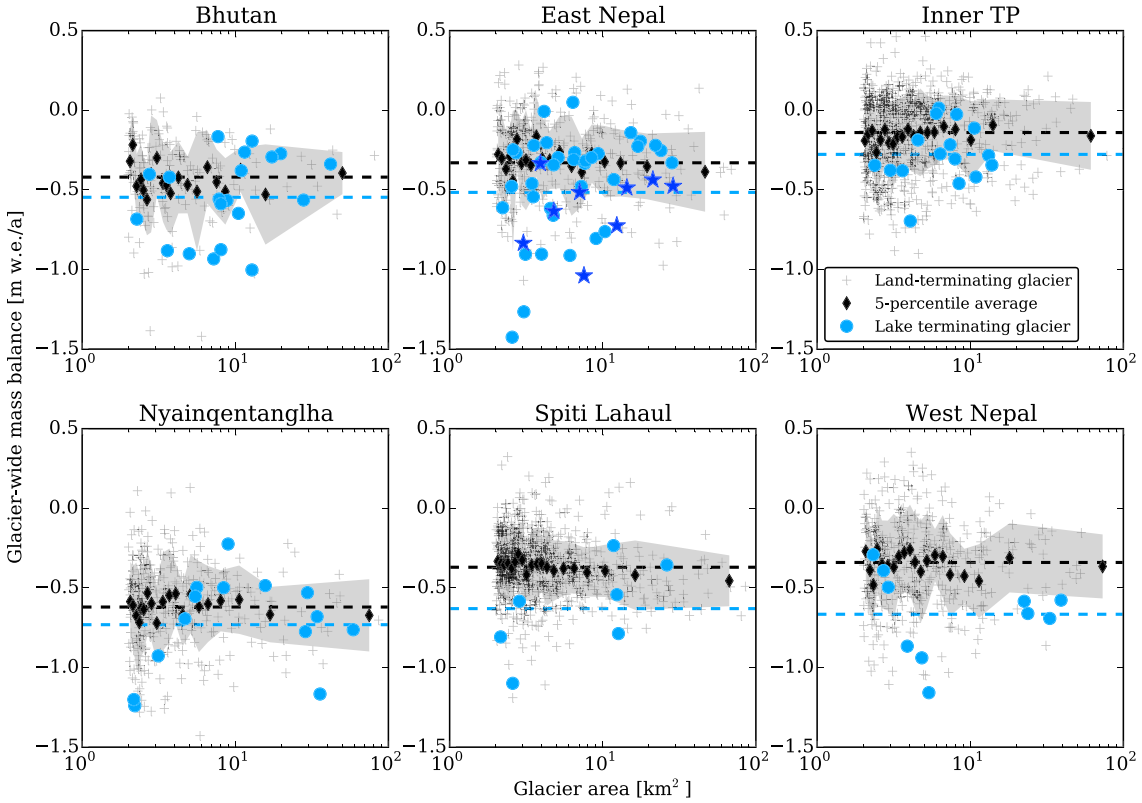

Figure 6. Glacier-wide mass balance as a function of glacier area. The black crosses represent the land terminating glaciers and the large blue dots the lake-terminating glaciers. The blue stars in East Nepal represent the nine lake-terminating glaciers studied by King et al. (2017). The black diamonds represent the 5-percentile averages of all glaciers. The gray envelope represents the ±one standard deviation from the mean. Note that for East Nepal, one lake-terminating glacier (with a size of 2.6 km^2) has a mass balance of −1.9 m w.e./year and therefore is missing on the plot. The horizontal dashed lines represent the regional averages for the lake-terminating glaciers (blue) and all the glaciers (black). TP = Inner Tibetan Plateau.

3.3. Influence of Proglacial Lakes on the Mass Balance Variability

In general, lake-terminating glaciers have more negative $\dot{M}$ than the regional average (Figure 6 and Table S13). They regularly lie further than one standard deviation from the mean. They have mean $\dot{M}$ that are between 0.11 and 0.32 m w.e./a more negative than the regional averages, in Nyainqentanglha and West Nepal, respectively (Table S13). If we consider the relative differences, they have mean $\dot{M}$ that are between 18% and 98% more negative than the regional averages, in Nyainqentanglha and inner TP, respectively (Table S13). It is noteworthy that the lake influence on $\dot{M}$ decreases with the glacier area, as the large lake-terminating glaciers tend to have $\dot{M}$ closer to the regional average than the small lake-terminating glaciers (Figure 6). The differences between $\dot{M}$ observed for lake-terminating glaciers and $\dot{M}$ predicted with the multivariate linear model based on a combination of four variables (see below and Table S13) are mostly negative (range: −0.44 to 0.07 m w.e./a), meaning that the excess mass loss is likely to be attributed to the presence of a lake at the glacier terminus and not to the glacier morphology (i.e., the fact that they often exhibit a gently sloped tongue at the terminus for instance).

3.4. Morphological Variables and Glacier Mass Balance Variability

For selected regions, the morphological variables have various influences on $\dot{M}$ and different correlations among each others (Figure 4). Note that we do not present the results for all the variables described in section 2. The aspect and area are not significant contributors to $\dot{M}$ for almost all of the regions (Tables S1–S12). The median elevation, minimum elevation, and maximum elevations are discarded because the mean elevation is a better predictor in most cases and is less sensitive to the quality of the input DEM than the maximum and minimum elevations.

First, we investigate which variables have a high correlation with $\dot{M}$. $\dot{M}$ has always a significant positive correlation (R ranging from 0.16 to 0.49 with $p < 0.001$) with the tongue slope (Figure 4), meaning the gentler the glacier slope, the more negative $\dot{M}$. Except for Spiti Lahaul and Pamir Alai, the mean elevation

Table 2
Results of the Multivariate Linear Regression to Explain the Glacier Mass Balance Variability for Each Region

Region	B	EN	HK	TP	Ka	Ku	N	P	PA	SL	TS	WN
Term. slope (−)	0.47	0.47	0.38	0.23	0.18	0.10	0.46	0.26	0.29	0.45	0.24	0.51
Mean elev. (−)	0.75	0.30	0.34	0.23	−0.34	0.21	−0.06	0.16	−0.19	0.17	0.47	0.18
DC (−)	0.09	0.00	0.13	−0.40	−0.16	−0.11	0.15	0.09	−0.23	0.06	0.12	0.12
Contrib. area (−)	0.37	0.11	0.07	0.17	−0.02	−0.10	−0.01	0.02	−0.07	0.09	−0.05	0.06
R^2	0.48	0.25	0.21	0.21	0.11	0.15	0.24	0.08	0.20	0.18	0.36	0.25
n	104	428	297	721	1,176	684	391	552	141	679	877	416
p <0.001		0.001 < p <0.01	0.01 < p <0.1	$p \geq 0.1$								

Note. The variables are standardized, and therefore, the coefficients associated with each variable are directly representative of their relative influence on the glacier mass balance variability. R^2 is the squared Pearson coefficient for the multivariate linear regression, including all the predictors. We reported the coefficients (α_i), colored according to the p values. The acronyms are the same ones as used in Figure 1, and n is the number of glaciers considered in this study for each region.

is significantly correlated with $\dot{M}$. This correlation is generally positive, with R ranging from 0.13 to 0.53 ($p < 0.01$ or $p < 0.001$), meaning the higher the glacier, the less negative $\dot{M}$. This correlation is negative for Karakoram and Nyainqentanglha. For five regions (East Nepal, Hindu Kush, Inner TP, Kunlun, and Pamir Alay), the DC is significantly and negatively correlated with $\dot{M}$, meaning the higher the percentage of debris cover area, the more negative the glacier mass balance. However, for the other regions, either it is the opposite (for Nyainqentanglha and Tien Shan) or the correlation is not significant. The avalanche contributing area is usually not significantly correlated with $\dot{M}$, except in Kunlun and inner TP, where it is negatively correlated with $\dot{M}$ (Tables S1–S12).

Second, we calculated a multivariate linear model, which explains 8% to 48% of $\dot{M}$ variability, based on a linear combination of four variables ignoring interaction between the variables (Table 2). The regions where the explained variability is the lowest are the Pamir, Karakoram, and Kunlun. The regions where the explained variability is the highest are the Bhutan and Tien Shan. Except for the Kunlun region, the tongue slope is always a significant predictor of $\dot{M}$ variability, and for 7 regions out of 12, it is the predictor which has the largest α_i, and consequently, the strongest influence on $\dot{M}$ variability. The mean elevation has a significant contribution to $\dot{M}$ variability for 10 regions out of 12 and has the largest α_i for four regions. The supraglacial debris cover has a significant contribution to $\dot{M}$ variability for four regions and is sometimes positive and sometimes negative. It has the largest α_i only for the inner TP, with a negative value. Again, this result is to be interpreted carefully, as the inner TP glaciers have only 3.2% of areal supraglacial debris cover on average. In the other regions, it has a small α_i compared with the other predictors. The avalanche contributing area is a significant contributor to $\dot{M}$ variability only for two regions. It has a small α_i (always less than half of the largest α_i in absolute value) compared with the other predictors (Table 2).

4. Discussion

4.1. Limitations of our Analysis

The statistical analysis presented here is sensitive to outliers, biases, and uncertainties in the data. The individual mass balance data have themselves a relatively high level of uncertainty with a median uncertainty of 0.22 m w.e./a (ranging from 0.14 to 0.89 m w.e./a), depending on the glacier area, on the proportion of the glacier surface surveyed, and on the number of DEMs available to extract a reliable rate of elevation change signal (Brun et al., 2017). The median uncertainty is slightly higher than the root mean square error of 0.17 m w.e./a found when comparing ASTER $\dot{M}$ with higher-resolution geodetic mass balances for 60 glaciers (Brun et al., 2017). In order to test the sensitivity of two important results to this uncertainty, we perform a Monte Carlo test. We randomly generate 1,000 new series of $\dot{M}$. For each glacier, we randomly perturb the value of $\dot{M}$ following a normal distribution centered on the original value, with a standard deviation equals to the uncertainty on $\dot{M}$. We then repeat the same analysis as described above to assess the robustness of the differences between the regional mean of debris-covered and debris-free glaciers (Table S14) and to assess the robustness of the percentage of variance explained by the multivariate linear model (Figure S5). Regarding the regional differences between debris-free and debris-covered glaciers, the results are very robust, as a large majority (expressed in percent) of perturbed simulations leads to the same conclusion in

terms of sign and significance of the difference (Table S14). Regarding the robustness of the percentage of the variance explained by the linear model, the results are less convincing, as the perturbed series systematically lead to lower R^2 (about ~0.1 lower on average), in particular for the Tien Shan and Nyainqentanglha (Figure S5).

The other data sources are also subject to uncertainty in the glacier delineation (Paul et al., 2013), which, in turn, introduces large uncertainties in the debris cover extent, as formerly glacierized areas, now free of glaciers, would be classified as debris-covered area. The overall accuracy of the glacier surface classification is 91% (Kraaijenbrink et al., 2017). Moreover, the avalanche contributing area is sensitive to the quality of the DEM used to determine the upstream area of each glaciers (Tribe, 1992). These intrinsic limitations should be kept in mind.

One of the major limitation of our work is the use of non independent variables as explanatory variables in the multiple linear regression model. The tongue slope and mean elevation are the best predictors of the mass balance variability. However, these variables correlate with each other and with the percentage of supraglacial debris cover and avalanche contributing area (Figure 4). This means that the influence of such correlated secondary predictors cannot be interpreted within the multiple linear regression model framework, and the univariate analysis (Tables S1–S12) is more relevant in these cases. An alternative would be to introduce interaction terms (defined as $\alpha_{i,j}x_i x_j$ in our framework) in the multiple linear model. More sophisticated approaches, such as a hierarchical Bayesian approach, could also help mitigate this issue, even though these approaches fail as well when the level of correlation among explanatory variables exceeds ~0.6 (e.g., Jomelli et al., 2015).

The separation of the glaciers into two distinct categories (debris-covered and debris-free glaciers) is somehow arbitrary, as there is a continuum between these categories. Nevertheless, the choice of different thresholds has a limited influence on the results (Figures 5, S3, and S4), and therefore, the classification is still insightful.

Another limitation of our study is the separation of glaciers into regions that we assumed climatically homogeneous. The regions considered in this study have a much larger spatial extent than the Swiss or French Alps (<300 and 200 km long, respectively), as they spread from ~300 km (Pamir) to more than 2,000 km (inner TP). Regional divisions remain arbitrary and alternative delineations could be provided, based on climate data clustering, for example. This is especially true for regions such as the Tibetan Plateau and the Tien Shan, where we group glaciers that are under very different climate influences (e.g., Sakai & Fujita, 2017).

4.2. Specificities of Debris-Covered Glaciers in Terms of Morphology and Mass Balance Variability

Our results show that debris-covered tongues can be generally characterized as flatter and located at lower elevations than debris-free tongues. Moreover, the avalanche contributing area correlates strongly with the percentage of debris cover, hinting that large part of the debris supply originates from the glacier upper reaches (e.g., Wirbel et al., 2018). These conclusions are in line with those of Scherler et al. (2011a), even though, contrary to them, we do not include ice surface velocity in our analysis. The availability of ice surface velocities for the entire ablation areas of HMA glaciers (Dehecq et al., 2019) will help to further test the hypothesis of Scherler et al. (2011a), who observed symmetrical distributions of surface velocity for the debris-free glaciers and asymmetrical distributions of surface velocity for the debris-covered glaciers.

We did not systematically observe less negative glacier-wide mass balances for debris-covered glaciers, compared with debris-free glaciers. At the same time, Nuimura et al. (2012), Gardelle et al. (2012, 2013), and Kääb et al. (2012) observed similar thinning rates for debris-free and debris-covered tongues, which is not inconsistent with our observations given that thinning rates are a result not only on point mass balance but also on emergence/submergence velocity (Brun et al., 2018).

Even though we did not document glacier terminus changes, it was already shown for selected regions of HMA that the debris-covered tongues experience less or no retreat compared with debris-free tongues (e.g., Scherler et al., 2011b; Xiang et al., 2018). However, debris-covered and debris-free glaciers have mostly similar $\dot{M}$, meaning that they have to respond through different mechanisms to climate changes. The debris-covered glaciers thin differently from the debris-free glaciers: debris-covered glacier thinning is distributed over their lower reaches independently of the elevation, whereas debris-free glaciers preferentially experience front retreat (Rowan, 2017; Rowan et al., 2015; Salerno et al., 2017). Consequently, the ice

dynamics play a major role for the evolution of debris-covered tongues, and the stable front positions of debris-covered glaciers should not be interpreted as balanced mass budget (Scherler et al., 2011b).

4.3. Proglacial Lake Influence on Glacier Mass Balance

In this study, we find that lake-terminating glaciers have $\dot{M}$ 18% to 98% more negative than the regional average. However, the lake influence depends on the glacier size and the lake's stage of development (Benn et al., 2012; King et al., 2017). Our more complete mass balance data set offers an opportunity to test the representativeness of the smaller glacier sample used in King et al. (2017). The glacier sample of King et al. (2017) has a mean $\dot{M}$ of -0.61 ± 0.11 m w.e./a (vs. -0.70 ± 0.27 m w.e./a in their study), which is slightly more negative than the average of all lake-terminating glaciers of East Nepal (Figure 6). The results presented in this study are a broad regional overview, and more studies should be conducted on specific lake-terminating glaciers to better understand the lake influence on the glacier dynamics and mass balance (King et al., 2018). Local studies are even more pressing because of the associated risk of GLOFs (Haritashya et al., 2018). In our study, we observe that there is no relationship between glacier-wide mass balances of lake-terminating glaciers and the degree of danger of the associated lakes.

4.4. Complex Influence of the Morphological Variables on the Glacier Mass Balance

The morphological variables explain 8% to 48% of $\dot{M}$ variance, with contrasted regional behaviors. Qualitatively, it seems that the regions where $\dot{M}$ is the most negative (Nyainqentanglha, Bhutan, and Tien Shan) are the regions where the morphological variables explain the largest part of the variance. Our interpretation of this observation remains rather speculative. A possibility is that morphological variables are linked to glacier response time and glacier mass balance sensitivity to climate change. Indeed, response times of glaciers with low slopes at their terminus, and in turn with slow dynamics, are longer than steep glaciers. Consequently, their geometry does not adapt quickly to changes in climate, they remain in imbalance for a longer time, and their mass balance is driven toward negative values explaining why the correlation between $\dot{M}$ and morphological variables such as the slope is high (Cuffey & Paterson, 2010). Similarly, glaciers lying at low elevations are expected to receive more precipitation and/or to have a larger accumulation basin than glaciers at high elevations, in order to balance higher ablation in the lower reaches. These glaciers have thus a larger mass turnover, and consequently, they are more sensitive to an increase in temperature (Oerlemans & Reichert, 2000).

Studies focusing in the Alps found comparable influences of morphological variables on $\dot{M}$ variability, although this region is climatically and topographically different from the regions of our study. In the Swiss Alps, Huss (2012) found that a combination of three variables (area, median glacier elevation, and slope of the tongue) explained 35% of the variance of a sample of 50 glacier mass balances averaged over 100 years. The explained variance reached 51% when using a combination of six variables (the former three variables, the latitude, the longitude, and the aspect). In the French Alps, Rabatel et al. (2016) found that the slope of the tongue and the glacier median elevation explained 25% of the variance of a sample of 30 glacier mass balances averaged over 31 years. The anticorrelation between $\dot{M}$ and the area was found only for glaciers smaller than 0.1 km^2 in the Alps, and above 0.1 km^2, the 1980–2010 mass balances of Swiss glaciers was relatively independent on glacier size (Fischer et al., 2015). Here we analyzed only glaciers larger than 2 km^2, which may explain why we did not find such a relationship.

The multiple correlations among the predictors complicate the interpretation of the results, but the multivariate linear model can partially separate the contribution of each predictor (Table 2). At first sight, the negative correlation between $\dot{M}$ and the supraglacial debris cover seems counter intuitive, because debris, when thick enough, is expected to insulate the glacier tongue and reduce ice ablation (e.g., Østrem, 1959; Vincent et al., 2016). However, this negative correlation is partially induced by the correlations between the debris cover and the mean elevation and tongue slope, which are themselves correlated with $\dot{M}$ (Figure 4). The multivariate linear model shows that the tongue slope and the mean elevation are the best predictors of $\dot{M}$. These findings can be interpreted similarly to a modeling study, which found higher mass balance sensitivity to an increase in temperature for debris-covered glaciers, than for debris-free glaciers (Huss & Fischer, 2016). The higher sensitivity of debris-covered glaciers and their more negative $\dot{M}$ (compared with debris-free glaciers) could be due to their typical settings at low elevation and their gentle tongue slope favoring high sensitivity to temperature changes and long response times (Huss & Fischer, 2016).

5. Conclusions

We assess the main morphological controls on glacier mass balances of HMA glaciers for the period 2000–2016. The morphological variables have contrasted influences over our 12 studied regions, and they explain 8% to 48% of the mass balance variability. The best predictors of this variability are the slope of the tongue and the mean elevation of the glaciers. The gentler the slope, the more negative the mass balance. Except for Spiti Lahaul and Pamir Alai, the higher the glacier, the less negative or the more positive its mass balance. The influence of the debris cover is less clear than that of the former predictors. In some regions, debris-covered glaciers have similar or more negative mass balances than debris-free glaciers, and for other regions, we observe the opposite. The influence of the debris is complicated to untangle from the effect of the other morphological variables, because heavily debris-covered tongues are often situated at lower elevation than debris-free tongues, where ablation is higher. Overall, we did not observe systematic differences between debris-free and debris-covered glaciers in terms of glacier mass balances.

Lake-terminating glaciers have more negative mass balances than the region averages. Nevertheless, this effect is not systematic, and specific studies need to be conducted on these glaciers to better quantify the lake influence and assess the GLOF hazard.

As the morphological variables explain only a limited fraction of the mass balance variability, we advocate for deeper investigations of the link between climatology, climate change, and glacier mass balance. First of all, climatically homogeneous regions have to be defined in an objective way. Once this step is achieved, it would be very interesting to investigate the glacier mass balance sensitivities to temperature and precipitation changes, in order to understand whether the recent mass changes can be attributed to contrasting climate sensitivity or to heterogeneous climate changes. However, this is a great challenge in HMA, since existing large-scale climate data sets do not accurately represent conditions at the glacier locations.

Acknowledgments
This work was supported by the French Space Agency (CNES). F. B. and P. W. acknowledge funding from the French Service d'Observation GLACIOCLIM and ANR-13-SENV-0005-04/05-PRESHINE. The glacier mass balances data are available through the World Glacier Monitoring Service database (https://wgms.ch/) and through the pangaea plateform (https://doi.pangaea.de/10.1594/PANGAEA.876545) for the rate of elevation change maps. The other data are accessible at http://mountainhydrology.org/data-nature-2017/, and the code used to generate them is available online (https://doi.org/10.5281/zenodo.2548690). We thank Yves Arnaud for providing expert knowledge in the debris-covered glacier classification. We thank three anonymous reviewers, the editor in chief, and the associate editor who provided comments that greatly improved this manuscript.

References

Akaike, H. (1974). A new look at the statistical model identification. *IEEE transactions on automatic control*, *19*(6), 716–723.

Basnett, S., Kulkarni, A. V., & Bolch, T. (2013). The influence of debris cover and glacial lakes on the recession of glaciers in Sikkim Himalaya, India. *Journal of Glaciology*, *59*, 1035–1046. https://doi.org/10.3189/2013JoG12J184

Benn, D., Bolch, T., Hands, K., Gulley, J., Luckman, A., Nicholson, L., et al. (2012). Response of debris-covered glaciers in the Mount Everest region to recent warming, and implications for outburst flood hazards. *Earth-Science Reviews*, *114*(1–2), 156–174. https://doi.org/10.1016/j.earscirev.2012.03.008

Bernhardt, M., & Schulz, K. (2010). SnowSlide: A simple routine for calculating gravitational snow transport. *Geophysical Research Letters*, *37*, L11502. https://doi.org/10.1029/2010GL043086

Bojinski, S., Verstraete, M., Peterson, T. C., Richter, C., Simmons, A., & Zemp, M. (2014). The concept of essential climate variables in support of climate research, applications, and policy. *Bulletin of the American Meteorological Society*, *95*(9), 1431–1443. https://doi.org/10.1175/BAMS-D-13-00047.1

Brun, F., Berthier, E., Wagnon, P., Kääb, A., & Treichler, D. (2017). A spatially resolved estimate of High Mountain Asia glacier mass balances from 2000 to 2016. *Nature Geoscience*, *10*, 668–673.

Brun, F., Wagnon, P., Berthier, E., Shea, J. M., Immerzeel, W. W., Kraaijenbrink, P. D. A., et al. (2018). Ice cliff contribution to the tongue-wide ablation of Changri Nup Glacier, Nepal, central Himalaya. *The Cryosphere*, *12*(11), 3439–3457. https://doi.org/10.5194/tc-12-3439-2018

Cogley, J. G., Hock, R., Rasmussen, L. A., Arendt, A. A., Bauder, A., Braithwaite, R. J., et al. (2011). Glossary of glacier mass balance and related terms. *IHP-VII Technical Documents in Hydrology*, *86*, 965.

Conrad, O., Bechtel, B., Bock, M., Dietrich, H., Fischer, E., Gerlitz, L., et al. (2015). System for Automated Geoscientific Analyses (SAGA) v. 2.1.4. *Geoscientific Model Development*, *8*(7), 1991–2007. https://doi.org/10.5194/gmd-8-1991-2015

Cuffey, K. M., & Paterson, W. S. B (2010). *The physics of glaciers*. Amsterdam: Academic Press.

Dehecq, A., Gourmelen, N., Gardner, A. S., Brun, F., Goldberg, D., Nienow, P. W., et al. (2019). Twenty-first century glacier slowdown driven by mass loss in High Mountain Asia. *Nature Geoscience*, *12*(1), 22–27. https://doi.org/10.1038/s41561-018-0271-9

Farr, T. G., Rosen, P. A., Caro, E., Crippen, R., Duren, R., Hensley, S., et al. (2007). The Shuttle Radar Topography Mission. *Reviews of Geophysics*, *45*, RG2004. https://doi.org/10.1029/2005RG000183

Fischer, M., Huss, M., & Hoelzle, M. (2015). Surface elevation and mass changes of all Swiss glaciers 1980–2010. *The Cryosphere*, *9*(2), 525–540. https://doi.org/10.5194/tc-9-525-2015

Forsythe, N., Fowler, H. J., Li, X.-F., Blenkinsop, S., & Pritchard, D. (2017). Karakoram temperature and glacial melt driven by regional atmospheric circulation variability. *Nature Climate Change*, *7*, 664–670. https://doi.org/10.1038/nclimate3361

Freeman, T. G. (1991). Calculating catchment area with divergent flow based on a regular grid. *Computers & Geosciences*, *17*(3), 413–422. https://doi.org/10.1016/0098-3004(91)90048-I

Gardelle, J., Berthier, E., & Arnaud, Y. (2012). Impact of resolution and radar penetration on glacier elevation changes computed from DEM differencing. *Journal of Glaciology*, *58*(208), 419–422. https://doi.org/doi:10.3189/2012JoG11J175

Gardelle, J., Berthier, E., Arnaud, Y., & Kääb, A. (2013). Region-wide glacier mass balances over the Pamir-Karakoram-Himalaya during 1999–2011. *The Cryosphere*, *7*(4), 1263–1286. https://doi.org/10.5194/tc-7-1263-2013

Gardner, A. S., Moholdt, G., Cogley, J. G., Wouters, B., Arendt, A. A., Wahr, J., et al. (2013). A reconciled estimate of glacier contributions to sea level rise: 2003 to 2009. *Science*, *340*, 852–857. https://doi.org/10.1126/science.1234532

Haritashya, U. K., Kargel, J. S., Shugar, D. H., Leonard, G. J., Strattman, K., Watson, C. S., et al. (2018). Evolution and controls of large glacial lakes in the Nepal Himalaya. *Remote Sensing*, *10*(5), 798. https://doi.org/10.3390/rs10050798

Herreid, S., & Pellicciotti, F. (2018). Automated detection of ice cliffs within supraglacial debris cover. *The Cryosphere*, *12*(5), 1811–1829. https://doi.org/010.5194/tc-12-1811-2018

Hocking, R. R. (1976). The analysis and selection of variables in linear regression. *Biometrics*, *32*(1), 1–49. https://doi.org/10.2307/2529336

Huss, M. (2012). Extrapolating glacier mass balance to the mountain-range scale: The European Alps 1900–2100. *The Cryosphere*, *6*(4), 713–727. https://doi.org/10.5194/tc-6-713-2012

Huss, M., & Fischer, M. (2016). Sensitivity of very small glaciers in the Swiss Alps to future climate change. *Frontiers in Earth Science*, *4*, 34. https://doi.org/10.3389/feart.2016.00034

Huss, M., Hock, R., Bauder, A., & Funk, M. (2012). Conventional versus reference-surface mass balance. *Journal of Glaciology*, *58*(208), 278–286. https://doi.org/10.3189/2012JoG11J216

Janke, J. R., Bellisario, A. C., & Ferrando, F. A. (2015). Classification of debris-covered glaciers and rock glaciers in the Andes of central Chile. *Geomorphology*, *241*, 98–121. https://doi.org/10.1016/j.geomorph.2015.03.034

Jomelli, V., Pavlova, I., Eckert, N., Grancher, D., & Brunstein, D. (2015). A new hierarchical Bayesian approach to analyse environmental and climatic influences on debris flow occurrence. *Geomorphology*, *250*, 407–421. https://doi.org/10.1016/j.geomorph.2015.05.022

Kääb, A., Berthier, E., Nuth, C., Gardelle, J., & Arnaud, Y. (2012). Contrasting patterns of early twenty-first-century glacier mass change in the Himalayas. *Nature*, *488*(7412), 495–498. https://doi.org/10.1038/nature11324

Kääb, A., Treichler, D., Nuth, C., & Berthier, E. (2015). Brief communication: Contending estimates of 2003–2008 glacier mass balance over the Pamir-Karakoram-Himalaya. *The Cryosphere*, *9*(2), 557–564. https://doi.org/10.5194/tc-9-557-2015

Kapnick, S. B., Delworth, T. L., Ashfaq, M., Malyshev, S., & Milly, P. C. D. (2014). Snowfall less sensitive to warming in Karakoram than in Himalayas due to a unique seasonal cycle. *Nature Geoscience*, *7*, 834–840. https://doi.org/10.1038/ngeo2269

King, O., Dehecq, A., Quincey, D., & Carrivick, J. (2018). Contrasting geometric and dynamic evolution of lake and land-terminating glaciers in the central Himalaya. *Global and Planetary Change*, *167*, 46–60. https://doi.org/10.1016/j.gloplacha.2018.05.006

King, O., Quincey, D. J., Carrivick, J. L., & Rowan, A. V. (2017). Spatial variability in mass loss of glaciers in the Everest region, central Himalayas, between 2000 and 2015. *The Cryosphere*, *11*(1), 407–426. https://doi.org/10.5194/tc-11-407-2017

Kraaijenbrink, P. D. A., Bierkens, M. F. P., Lutz, A. F., & Immerzeel, W. W. (2017). Impact of a global temperature rise of 1.5 degrees Celsius on Asia glaciers. *Nature*, *549*, 257–260. https://doi.org/10.1038/nature23878

Maharjan, S. B., Mool, P. K., Lizong, W., Xiao, G., Shrestha, F., Shrestha, R., et al. (2018). The status of glacial lakes in the Hindu Kush Himalaya (*Tech. rep.*) Kathmandu: ICIMOD.

Maussion, F., Scherer, D., Mlg, T., Collier, E., Curio, J., & Finkelnburg, R. (2014). Precipitation seasonality, and variability over the Tibetan Plateau as resolved by the High Asia Reanalysis. *Journal of Climate*, *27*(5), 1910–1927. https://doi.org/10.1175/JCLI-D-13-00282.1

Nicholson, L., & Benn, D. I. (2006). Calculating ice melt beneath a debris layer using meteorological data. *Journal of Glaciology*, *52*, 463–470. https://doi.org/10.3189/172756506781828584

Nuimura, T., Fujita, K., Yamaguchi, S., & Sharma, R. R. (2012). Elevation changes of glaciers revealed by multitemporal digital elevation models calibrated by GPS survey in the Khumbu region, Nepal Himalaya, 1992–2008. *Journal of Glaciology*, *58*(210), 648–656. https://doi.org/10.3189/2012JoG11J061

Oerlemans, J., & Reichert, B. K. (2000). Relating glacier mass balance to meteorological data by using a seasonal sensitivity characteristic. *Journal of Glaciology*, *46*(152), 1–6. https://doi.org/10.3189/172756500781833269

Østrem, G. (1959). Ice melting under a thin layer of moraine, and the existence of ice cores in moraine ridges. *Geografiska Annaler*, *41*(4), 228–230.

Paul, F., Barrand, N. E., Baumann, S., Berthier, E., Bolch, T., Casey, K., et al. (2013). On the accuracy of glacier outlines derived from remote-sensing data. *Annals of Glaciology*, *54*, 171–182. https://doi.org/10.3189/2013AoG63A296

Paul, F., & Haeberli, W. (2008). Spatial variability of glacier elevation changes in the Swiss Alps obtained from two digital elevation models. *Geophysical Research Letters*, *35*, L21502. https://doi.org/10.1029/2008GL034718

Pfeffer, W. T., Arendt, A. A., Bliss, A., Bolch, T., Cogley, J. G., Gardner, A. S., et al. (2014). The Randolph Glacier Inventory: A globally complete inventory of glaciers. *Journal of Glaciology*, *60*, 537–552. https://doi.org/10.3189/2014JoG13J176

Quincey, D. J., Richardson, S. D., Luckman, A., Lucas, R. M., Reynolds, J. M., Hambrey, M. J., & Glasser, N. F. (2007). Early recognition of glacial lake hazards in the Himalaya using remote sensing datasets. *Global and Planetary Change*, *56*, 137–152. https://doi.org/10.1016/j.gloplacha.2006.07.013

Rabatel, A., Dedieu, J. P., & Vincent, C. (2016). Spatio-temporal changes in glacier-wide mass balance quantified by optical remote sensing on 30 glaciers in the French Alps for the period 1983–2014. *Journal of Glaciology*, *62*(236), 1153–1166. https://doi.org/10.1017/jog.2016.113

Rabatel, A., Letréguilly, A., Dedieu, J.-P., & Eckert, N. (2013). Changes in glacier equilibrium-line altitude in the western Alps from 1984 to 2010: Evaluation by remote sensing and modeling of the morpho-topographic and climate controls. *The Cryosphere*, *7*(5), 1455–1471. https://doi.org/10.5194/tc-7-1455-2013

Röhl, K. (2006). Thermo-erosional notch development at fresh-water-calving Tasman Glacier, New Zealand. *Journal of Glaciology*, *52*(177), 203–213. https://doi.org/10.3189/172756506781828773

Rolstad, C., Haug, T., & Denby, B. (2009). Spatially integrated geodetic glacier mass balance and its uncertainty based on geostatistical analysis: Application to the western Svartisen ice cap, Norway. *Journal of Glaciology*, *55*(192), 666–680. https://doi.org/10.3189/002214309789470950

Rowan, A. V. (2017). The 'Little Ice Age' in the Himalaya: A review of glacier advance driven by Northern Hemisphere temperature change. *The Holocene*, *27*, 292–308. https://doi.org/10.1177/0959683616658530

Rowan, A. V., Egholm, D. L., Quincey, D. J., & Glasser, N. F. (2015). Modelling the feedbacks between mass balance, ice flow and debris transport to predict the response to climate change of debris-covered glaciers in the Himalaya. *Earth and Planetary Science Letters*, *430*, 427–438. https://doi.org/10.1016/j.epsl.2015.09.004

Sakai, A., & Fujita, K. (2017). Contrasting glacier responses to recent climate change in High-Mountain Asia. *Scientific Reports*, *7*(1), 13,717. https://doi.org/10.1038/s41598-017-14256-5

Salerno, F., Thakuri, S., Tartari, G., Nuimura, T., Sunako, S., Sakai, A., & Fujita, K. (2017). Debris-covered glacier anomaly? Morphological factors controlling changes in the mass balance, surface area, terminus position, and snow line altitude of Himalayan glaciers. *Earth and Planetary Science Letters*, *471*, 19–31. https://doi.org/10.1016/j.epsl.2017.04.039

Scherler, D., Bookhagen, B., & Strecker, M. R. (2011a). Hillslope-glacier coupling: The interplay of topography and glacial dynamics in High Asia. *Journal of Geophysical Research*, *116*, F2. https://doi.org/10.1029/2010JF001751

Scherler, D., Bookhagen, B., & Strecker, M. R. (2011b). Spatially variable response of Himalayan glaciers to climate change affected by debris cover. *Nature Geoscience*, *4*, 156–159. https://doi.org/10.1038/ngeo1068

Shean, D. (2017). *High Mountain Asia 8-meter DEM mosaics derived from optical imagery, version 1*. Boulder, Colorado USA: NASA National Snow and Ice Data Center Distributed Active Archive Center. https://doi.org/10.5067/KXOVQ9L172S2[Accessed in, March 2019.

Thompson, S. S., Benn, D. I., Dennis, K., & Luckman, A. (2012). A rapidly growing moraine-dammed glacial lake on Ngozumpa Glacier, Nepal. *Geomorphology*, *145*, 1–11. https://doi.org/10.1016/j.geomorph.2011.08.015

Tribe, A. (1992). Automated recognition of valley lines and drainage networks from grid digital elevation models: A review and a new method. *Journal of Hydrology*, *139*(1), 263–293. https://doi.org/10.1016/0022-1694(92)90206-B

Vincent, C., Fischer, A., Mayer, C., Bauder, A., Galos, S. P., Funk, M., et al. (2017). Common climatic signal from glaciers in the European Alps over the last 50 years. *Geophysical Research Letters*, *44*, 1376–1383. https://doi.org/10.1002/2016GL072094

Vincent, C., Wagnon, P., Shea, J. M., Immerzeel, W. W., Kraaijenbrink, P., Shrestha, D., et al. (2016). Reduced melt on debris-covered glaciers: Investigations from Changri Nup Glacier, Nepal. *The Cryosphere*, *10*(4), 1845–1858. https://doi.org/10.5194/tc-10-1845-2016

Wirbel, A., Jarosch, A. H., & Nicholson, L. (2018). Modelling debris transport within glaciers by advection in a full-Stokes ice flow model. *The Cryosphere*, *12*(1), 189–204. https://doi.org/10.5194/tc-12-189-2018

Xiang, Y., Yao, T., Gao, Y., Zhang, G., Wang, W., & Tian, L. (2018). Retreat rates of debris-covered and debris-free glaciers in the Koshi River Basin, central Himalayas, from 1975 to 2010. *Environmental Earth Sciences*, *77*(7), 285.

Zhang, G., Yao, T., Shum, C. K., Yi, S., Yang, K., Xie, H., et al. (2017). Lake volume and groundwater storage variations in Tibetan Plateau's endorheic basin. *Geophysical Research Letters*, *44*, 5550–5560. https://doi.org/10.1002/2017GL073773